Ecohydrology

WILEY

RESEARCH ARTICLE OPEN ACCESS

The Space–Time Representation of Extraordinary Rainfall Events

Salvatore Manfreda

Department of Civil, Architectural and Environmental Engineering, University of Naples Federico II, Naples, Italy

Correspondence: Salvatore Manfreda (salvatore.manfreda@unina.it)

Received: 11 January 2024 | **Revised:** 17 July 2024 | **Accepted:** 6 November 2024

Funding: This work was supported by European Commission.

Keywords: extraordinary events | rainfall statistics | space–time Poisson models

ABSTRACT

Extraordinary events are rarely observable in a single rainfall gauge, and this make extremely challenging the correct prediction of their arrivals. However, it may be possible to develop a more robust approach by employing a space–time modelling scheme that is able to capture the spatial dynamics of such phenomena. Therefore, a space–time Poisson model of rainfall cells with circular shape and random depth has been exploited for the first time to interpret the behaviour of this family of extraordinary events. This category of events that may be connected to larger meteorological phenomena not necessarily connected with local heterogeneity of the landscape. Following the identification of the observed extraordinary event across southern Italy, six zones with significantly different dynamics in terms of the frequency of such extremes were identified. Subsequently, a simple mathematical representation was adopted to calibrate the model parameters, leading to an estimate of regional probability distributions defined on the space–time occurrences of extraordinary events over homogeneous zones. The approach allows to overcome the limitations posed by point observations allowed the definition of a probability distribution that pertains to an entire area rather than just a point. The obtained quantiles of rainfall estimated seems to align well with the upper bound of the probability distribution of the annual maxima observed over the areas of interests.

1 | Introduction

Understanding and interpreting rainfall extremes poses a formidable challenge in hydrology, primarily due to the complexity of the atmospheric processes, but also for the limited observations available (Thompson et al. 2013; Fowler et al. 2021). Rainfall events constitute intricate phenomena evolving across different scales (e.g., Emmanouil et al. 2022), which require a significant monitoring effort that is not properly addressed by a sparse rainfall network. Current monitoring networks often underestimate rainfall events. Interpolation schemes typically show lower variance in the interpolated field compared to the original point data. Moreover, for high precipitation events, the maximum precipitation in the interpolated field usually aligns with an observation location, which is unrealistic (e.g., Bárdossy and Anwar 2023).

The introduction of radar networks offers significant advantages in terms of temporal and spatial coverage compared to most rain gauge networks (e.g., Overeem, Buishand, and Holleman 2009). While radar data has shown great potential for rainfall analysis, it also has limitations, particularly in interpreting rainfall quantiles. In fact, radar data tends to overestimate high extremes and requires bias correction (Goudenhoofdt, Delobbe, and Willems 2017). Additionally, weather radar averages precipitation over areas typically of one km^2 smoothing the within pixel variability. Studies have found that the mean areal extreme rainfall derived from radar underestimates extreme values at point locations within the radar pixel by about 70% on average (Peleg et al. 2018).

An alternative for a refinement of rainfall measurements is represented by the use of innovative sensors and network of private users. Crowd-sourced data from private sensors, smartphones, surveillance cameras, and other devices provide an unprecedented density of measurements. This enhanced accuracy helps to better describe the spatial structure of rainfall events, with measurements that can be easily filtered and validated, creating a dense observation network (Yang and Ng 2017; de Vos et al. 2019; Manfreda et al. 2024). However, there is still a lack of long-term series capable of describing and interpreting the dynamics of rare rainfall events.

In this context, there is a specific class of hydrological events that deserve more attention and dedication, which is represented by the extraordinary events (or outliers). These events are rarely observed especially at a point scale and for this reason, several approaches have been developed to overcome the limited observations available. For instance, regional methods tend to tackle this issue clustering group of stations based on local statistics in order to build a regional probability distribution (e.g., Hosking and Wallis 1988; Schaefer 1990; Hanson and Vogel 2008; Lima et al. 2021). Within this context, the well-known Generalized Extreme Value (GEV) model (Jenkinson 1955) and Two-Component Extreme Value (TCEV) distribution (Rossi, Fiorentino, and Versace 1984) has been widely applied exploiting regional methods.

The TCEV distribution is obtained as a mixture of two processes exponentially distributed and with Poisson occurrences. These two populations consist of an ordinary component, more frequent and less severe in intensity, and an extraordinary component, responsible for generating the rarer but more extreme values. The strength of the TCEV model lies in its capability to predict the frequency of rainfall events with diverse meteorological characteristics without the need for prior classification based on meteorological criteria. TCEV has been widely used in several studies around the world (e.g., Connell and Pearson 2001; Caporali, Chiarello, and Petrucci 2018; Benito et al. 2020; Campos-Aranda 2022) and also for at-site studies on time series longer than 50 years (Totaro et al. 2024). In addition, it is worth mentioning that a user-friendly tool was recently introduced by De Luca and Napolitano (2023) for the use of the TCEV distribution along with others such as the EV1 and GEV.

In this context, an interesting contribution was given by Pelosi et al. (2020) that attempted to describe the behaviour of extraordinary events by measuring the proportion of such events within the annual maxima and exploiting the conditional distribution of annual maxima when extraordinary events occur. This method was strongly motivated by the perception that a certain class of extreme events is induced by a specific category of meteorological events, which may have dynamics completely different from other ordinary events. An example of this is represented by the Medicanes (e.g., Romero and Emanuel 2013; Romera et al. 2017).

The conceptual foundation of the present manuscript stems from the idea of utilizing a space–time Poisson representation of rainfall cells to characterize extraordinary events. Although constrained by the limited number of observations in our time-series, the adoption of a space–time model offers potential in augmenting observations in space, thereby enhancing our predictive capabilities for extraordinary events.

This work's conceptualization is deeply rooted in earlier research collaborations with Ignacio Rodriguez-Iturbe from 2004 to 2006, as evidenced by studies such as Isham et al. (2005), Rodríguez-Iturbe et al. (2006), and Manfreda and Rodrìguez-Iturbe (2006). Building upon this foundation, Fabio Rossi's exploration of extraordinary events trading space versus time (Pelosi et al. 2020) inspired a new strategy. Leveraging the rainfall model developed by Cox and Isham (1988), we present a comprehensive approach to characterize extraordinary rainfall events using an extensive dataset from southern Italy.

2 | Space–Time Rainfall Model

Spatio-temporal stochastic rainfall models offer the possibility of interpreting physical processes with a mathematical formalism that summarizes rainfall characteristics in a few parameters (Onof et al. 2000). Among others, Poisson-cluster processes represent a well-established schematization where storms arrive according to a Poisson process and are represented by clusters of rainfall cells with centres randomly located in space and time (e.g., Cox and Isham 1988; Kavvas and Delleur 1981; Waymire and Gupta 1981; Ramirez and Bras 1985; Istok and Boersma 1989). Rainfall cells can be characterized by random dimensions, lifetimes, velocities, and intensities.

This category of models is based on the work of Rodriguez-Iturbe, Cox, and Isham (1987) and, over time, has been exploited in several hydrological applications (e.g., Cowpertwait 1994, 1995, 1998; Cowpertwait and O'Connell 1997; Cowpertwait, 1997; Cowpertwait, Kilsby, and O'Connell 2002; Chen et al. 2021; Diez-Sierra, Navas, and del Jesus 2023).

Within this context, it is particularly relevant the study by Cowpertwait (1994) that developed an at-site rainfall stochastic model, in which each storm is characterized by a cluster of rain cells, with each cell having a random exponential lifetime and a random intensity. The local Poisson-cluster processes model has been generalized to consider that generated cells could be of n types; in particular, "heavy" or "light" categories have been analysed, with heavy cells having a shorter expected duration than the light ones. Thereafter, the proposed model was improved by Cowpertwait (1995) in order to obtain the generalized spatial–temporal Neyman–Scott model, a two-dimensional (space and time) model based on a clustered point process. This model has been implemented and tested in storm sewer rehabilitation studies in the UK (Cowpertwait et al. 1996). In detail, the model was regionalised over the area by regressing estimates (related to each time-series) of the model parameters on site variables. A related study was carried out by Cowpertwait and O'Connell (1997) by analysing the spatial variation of the patterns of two rain cell categories, i.e., stratiform and convective. This model has also been used to describe rainfall extremes in regional studies (Cowpertwait, Kilsby, and O'Connell 2002). In a more operative context, these models have been further explored for continuous hydrological modelling, obtaining good reconstructions of flow duration and flood frequency curves (Chen et al. 2021).

Following the formalism introduced by Cox and Isham (1988), the rainfall process is modelled as storms arriving in a Poisson process in space and time. The original model was characterized by storm events of circular shape with a random radius, duration, intensity and velocity.

In the present case, the model is similar but the storm (e.g., cells) has zero velocity and storm duration is assumed fixed, given that the variables of interest are the annual maxima of fixed duration. The model is thus characterized by three parameters assumed to be independent from storm to storm: the rate of rainy cells in space and time λ_R, the rain cell radius R and the rainfall depth X. The model although highly idealized allows the mathematical tractability of the resulting spatial statistics of the resulting process.

In order to keep the number of parameters to a minimum we will assume that the random variables R and X are exponentially distributed. The mean of the rainfall intensity process Y(0,t) is given by:

$$E[Y(0,t)] = \lambda_R E[DA]E[X] \tag{1}$$

where: λ_R is the rate of cells per unit time and area, E[DA] is the mean value of the rainfall cells and E[X] is the mean rainfall depth within each cell. For sake of simplicity and consistency with available data, the rainfall duration will be assumed fixed.

In addition, the mean rate of the process in time can be estimated as:

$$E[N(t)] = \lambda_R E[DA] \tag{2}$$

This model has been used in several applications for the description of daily rainfall processes and for the construction of soil moisture models with the aim to explore the spatial dynamics of soil moisture (see Isham et al. 2005; Rodríguez-Iturbe et al. 2006; Manfreda and Rodrìguez-Iturbe 2006; Nordbotten, Rodriguez-Iturbe, and Celia 2006).

3 | The Methodology

The proposed Space–time Maxima Model (STMM) utilizes the space–time rainfall scheme introduced by Cox and Isham (1988) with some simplifying assumptions. Surprisingly, this schematization appears suitable for describing hydrological extremes, especially extraordinary events. The STMM's parameters were estimated using the available rainfall dataset, which has some limitations but serves as a valuable reference for the present study.

The first step of the procedure involves identifying the threshold that distinguishes between ordinary and extraordinary observations. This task was carried out by applying the mathematical formulations of the TCEV, explicitly assuming that the probability distribution of extremes arises from the mixture of two populations. Therefore, this section will briefly introduce the TCEV, the threshold estimation strategy, and subsequently, the methodology adopted to extrapolate the STMM parameters.

3.1 | Identification of Extreme Events

Another crucial step of this approach is represented by the identification of extraordinary events. In this context, the well-known Two Component Extreme Value (TCEV) probability distribution proposed by Rossi, Fiorentino, and Versace (1984) can be beneficial. This distribution is based on the concept that natural extremes may result from the combination of two families of values associated with different meteorological phenomena: ordinary and extraordinary or outliers.

Applying the analytical formulation of the TCEV model, it becomes possible to objectively determine the rainfall threshold that distinguishes the ordinary component from the extraordinary one, as suggested by Beran, Hosking, and Arnell (1986).

Recalling the analytical expression of the TCEV:

$$P(Y \le y) = e^{\left(-\Lambda_1 e^{\left(-\frac{y}{\theta_1}\right)} - \Lambda_2 e^{\left(-\frac{y}{\theta_2}\right)}\right)} \tag{3}$$

where: Λ_1 and Λ_2 represents the annual expected number of rainfall events belonging, respectively, to the ordinary and the extra-ordinary component; θ_1 and θ_2 represents the expected value of the two populations. Therefore, the parameters of this distribution have a clear physical meaning.

The distribution can be rewritten adopting the so-called "shape" parameters:

$$\theta_* = \frac{\theta_2}{\theta_1} \quad \text{and} \quad \Lambda_* = \frac{\Lambda_2}{\Lambda_1^{\frac{1}{\theta_*}}} \tag{4}$$

The Cumulative Density Function (CDF) can be expressed as a function of the reduced variable $X = \frac{Y}{\theta_1} - \ln(\Lambda_1)$:

$$P(X \le x) = e^{\left(-e^{(-x)} - \Lambda_* e^{\left(-\frac{x}{\theta_*}\right)}\right)} \tag{5}$$

The TCEV distribution is characterized as the maximum of two independently distributed extreme value type 1 (EV1) variables. The proportion of data values distinguishing between the two populations (ordinary and extraordinary) can be derived using the theoretical formulation proposed by Beran, Hosking, and Arnell (1986). This proportion p is:

$$p = -\frac{\Lambda_*}{\theta_*}\sum_{j=0}^{\infty}\frac{(-1)^j}{j!}\Lambda_*^{\,j}\Gamma\left(\frac{j+1}{\theta_*}\right) \tag{6}$$

where θ_* and Λ_* are the TCEV shape parameters and Γ( ) is the gamma function. The above formulation has been also adopted by Boni, Parodi, and Rudari (2006) to explore the seasonality of extraordinary events.

3.2 | Probability Distribution of Rainfall Depth

The probability distribution of the variable (y-s) was observed to be exponentially distributed with a mean equal to E[Y] – s. Therefore, the probability distribution of rainfall intensities, y, assume the following form:

$$p(y) = \frac{1}{E[Y] - s} e^{\left(-\frac{y-s}{E[Y]-s}\right)} \tag{7}$$

The phenomena of extraordinary rainfall events belonging to the family of extraordinary events can be described with the Poisson process described with a distribution of the rainfall depth distributed according to an exponential distribution. The CDP of the compound Poisson process with rate λ assumes the following form:

$$P(Y \leq y) = e^{\left(-\lambda\, e^{\left(-\frac{y-s}{E[Y]-s}\right)}\right)} \tag{8}$$

4 | Results

4.1 | The Study Area and the Dataset

The study area encompasses a significant portion (20%) of the Italian peninsula, covering the regions of Apulia (with a surface area of 19,500 km^2), Basilicata (10,000 km^2), Calabria (15,000 km^2), Campania (13,500 km^2), and Molise (4437 km^2). Situated within the Mediterranean basin, it is bordered by the Adriatic Sea to the east, the Ionian Sea to the southeast, and the Tyrrhenian Sea to the west. The region's topography is intricately shaped by the north-to-south Apennine chain, contributing to a complex orography.

The rainfall database used was compiled by Avino, Cimorelli, et al. (2024) and comprises approximately 910 rain gauges. These include all SIMN stations that have been operated over the territory throughout time and the newly installed rainfall stations managed by Civil Protection, as well as gauges from agrometeorological monitoring networks. The database encompasses annual rainfall maxima for sub-daily intervals (ranging from 1 to 24 h) covering the period from 1970 to 2020.

Given the strong discontinuity of time series, the dataset has been reconstructed by balancing the numerosity of the time series and reconstruction error using a procedure well-described in the work by Avino et al. (2021). The entire database is available online in the dataset published by Avino, Pianese, and Manfreda (2024).

Based on the recent study by Avino, Cimorelli, et al. (2024), there is a notable increase in annual rainfall maxima observed over shorter durations in various locations. However, these trends disappear for durations longer than 12 h. Therefore, it appears reasonable to consider the time series of annual maxima at 24 h as stationary.

4.2 | Selection of the Extraordinary Events

Given the speculative aim of the manuscript and the limited information available on the extraordinary component of rainfall events, the underlining assumption adopted is that the two rainfall processes are strongly independent, with the second component more likely to be less affected by local factors. Therefore, all stations have been analysed as a single time series assuming that the second component can be estimated without any distinction between areas.

In this regard, Pelosi et al. (2020) adopted a similar approach identifying the threshold by visual inspection of the probability distribution of daily rainfall. In the present case, the TCEV is adopted, assuming that the extraordinary component may have the same characteristics at all sites.

Therefore, the discriminant between ordinary and extraordinary events can be defined adopting the probability term introduce in Equation 6 of Section 3.1. Specifically, the probability distribution of annual maxima across the entire study area has been utilized to identify a threshold "s", as reported in the graph in Figure 1A. This graph represents the probability distribution of all time-series of the rainfall event at 24 h observed or reconstructed over the entire southern Italy.

It is worthy to mention that only on 609 of the 911 stations available, the threshold s is of 112 mm was reached and passed. The total number of extraordinary events available in the database

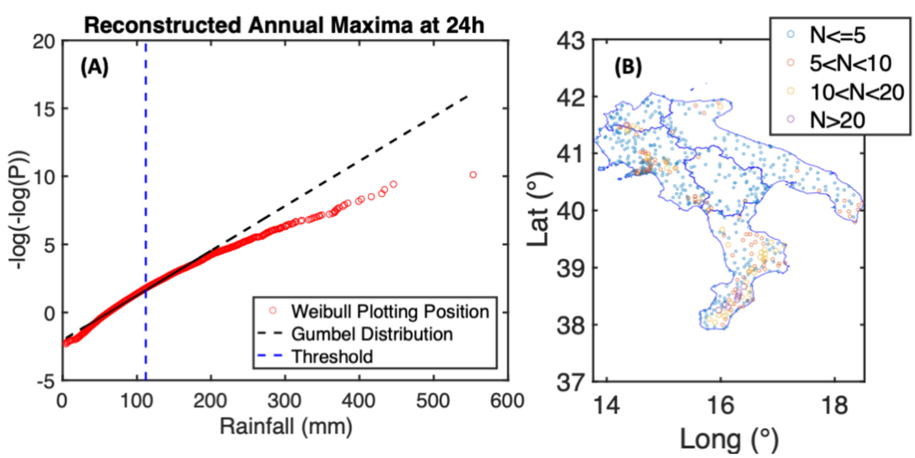

FIGURE 1 | Annual maxima identification of extraordinary events: A) Cumulative probability distribution of the annual maxima at 24 h measured over southern Italy. B) Number of extraordinary events observed in each station of the study area.

is of about 2458 events distributed quite heterogeneously along the entire territory. Their distribution is depicted in Figure 1B, which allows to immediately discern the spatial pattern of such phenomena, which exhibits a clear gradient across the region.

The obtained threshold may certainly represent an approximation, but it is interesting to observe later in this manuscript that the results of the obtained probability distribution are consistent with the results from local estimates. Additionally, it is worth mentioning that Pelosi et al. (2020) adopted a similar approach, identifying the threshold through visual inspection of the probability distribution of daily rainfall over the entire Italian territory. They selected a threshold of 250 mm, which was identified as the parameter at which there was a significant departure of observed frequencies from the fitted probability model.

4.2.1 | Probability Density Function of Rainfall Above the Thresholds

The threshold allows us to explore and characterize the probability distribution of the rainfall events above this threshold.

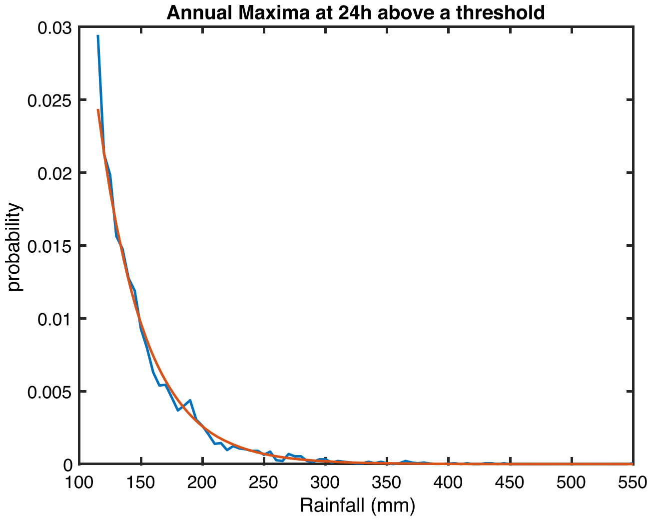

FIGURE 2 | Probability density function of rainfall intensities above the threshold of 112 mm/day obtained using all 910 rain gauges of the area.

Such a distribution can be described by Equation 6. The reliability of this distribution is tested in Figure 2, where the probability distribution of rainfall intensities above the threshold, s, is represented along with the mathematical function given above. The function refers to all the rainfall values recorded within the area of interest.

4.3 | Rainfall Data Processing

The estimation of parameters for the space–time Poisson model involved a series of approximations, introducing necessary errors for testing the overarching concept. It is crucial to acknowledge that the rainfall dataset exclusively consists of annual maxima without specific dates, making the reconstruction of historical rainfall events unfeasible. However, the likelihood of extraordinary rainfall events from the same year and in close proximity belonging to different events is minimal. Therefore, the available annual maxima were utilized to extrapolate cells of extraordinary events that occurred over the considered time window. This was done by assuming that annual maxima above a threshold “s”, identifying extraordinary events, could be associated with a single extraordinary event.

With this aim, a multi-step approach was adopted, and it is depicted in Figure 3.

- Firstly, annual rainfall time series were utilized to generate 2D rainfall fields using the Inverse Distance Weighting (IDW) method each year (using an exponent equal two for the distance and number of neighbours is set equal eight). An example of 2D reconstruction is given in Figure 3A.
- Subsequently, the rainfall map has been segmented in cells above a given threshold, which will be identified in Section 4.2. The rainfall cells surpassing a predefined threshold were isolated and characterized. An example of this second step is given in Figure 3B where nine cells with different intensities and sizes have been identified.
- The sequence of extraordinary cells observed in space has been employed to characterize the spatial frequency of exceptional events. This information has, in turn, been utilized for identifying homogeneous areas. Figure 3C provides

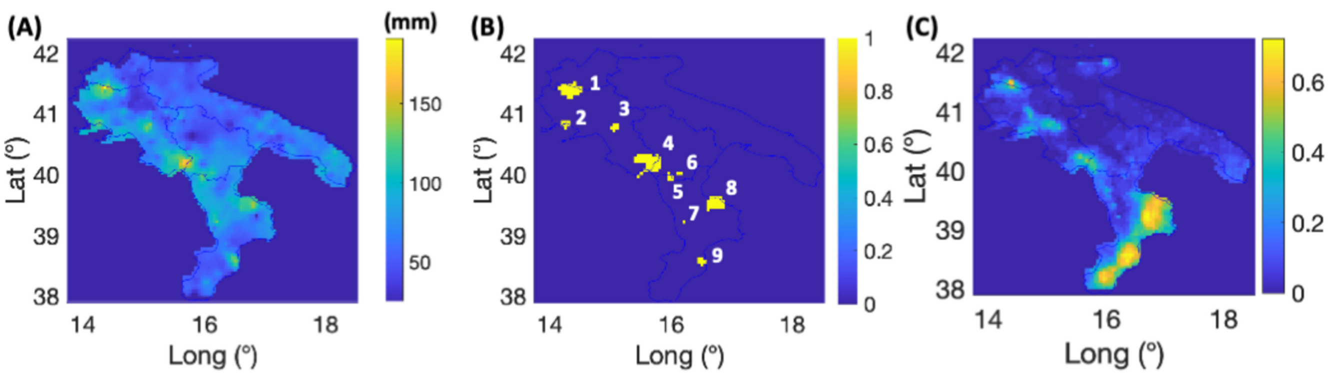

FIGURE 3 | Example of extrapolation of the spatial characteristics of rainfall cell associated to extraordinary events: A) Example of interpolated rainfall field of annual maxima for a given year, 1980; B) Example of identified cells with rainfall above the threshold value s in the year 1980. C) Frequency of extraordinary events observed over the time-window considered (1970–2020).

an illustrative example of the results obtained across the entire temporal window under consideration.

- Then, the study area was classified into six regions employing k-means clustering based on the frequency of extraordinary events (see Figure 4).
- Finally, within each homogeneous region, the intensity and size of rainfall cells associated with extraordinary events were quantified, facilitating the derivation of parameters for the Poisson process.

Based on the above procedure, six regions were identified based on the frequency of extraordinary events. Among these, an area along the Ionian coast stands out, exhibiting a significantly high number of occurrences of extraordinary events (Zone 4). Additionally, three other subregions also demonstrate a relatively high number of extraordinary events: the Park of Matese (Zone 1), the Sorrento Peninsula (Zone 2), and the Gulf of Policastro (Zone 3). The remaining two zones (5 and 6) cover the remaining territory, with the zone 5 identifying the most internal areas where the number of extraordinary events is limited and finally the zone 6 representative of coastal areas without significant relief.

These areas are depicted in Figure 4, where it is possible to observe the strong impact of the Apennine chain on the observed patterns. It is worthy to observe how the Calabria region is separated in two regions with a limit that goes along the relief line (Versace et al. 1989). In addition, regional studies on the Basilicata region also highlighted also identified a hotspot localized next to the Tyrrhenian coast similar to the one identified herein as zone 3 (see Claps and Fiorentino 2001).

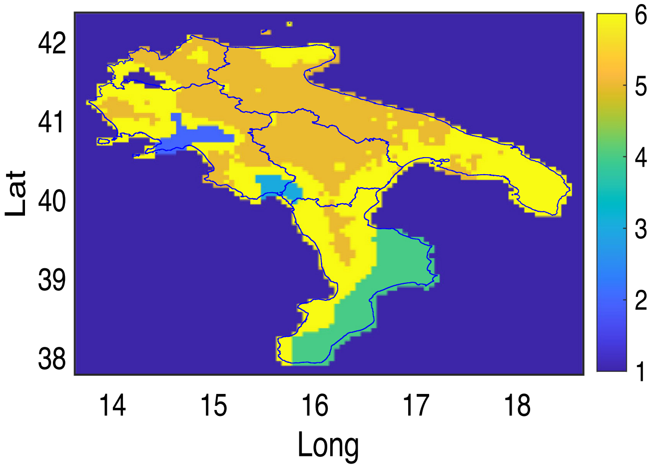

FIGURE 4 | The rainfall zones identified with a clustering approach based on the frequency of extraordinary rainfall events applied over the Southern Italy District. The spatial resolution adopted for the analysis was 5.5 km.

These six regions exhibit clear and significant differences, as evidenced by the model parameters obtained for each area. These parameters highlight a noticeable distinction not only in the frequency of extraordinary events, but also in the configuration of rainfall cells. It is worth noting that, concerning the latter aspect, an ideal dataset for a comprehensive study like this would consist of an extended record of radar observations possibly calibrated with ground observations. Such a dataset could contribute to achieving a more robust reconstruction of the characteristics of extraordinary events. While maps for these observations are available, they cover only a short period, and in most cases, they require time-consuming calibration. Therefore, it is acknowledged that the analysis presented here could certainly be refined. Nevertheless, it serves as an interesting starting point for a quantitative characterization of the right tail of the probability distribution of extreme events.

Building upon the six, it became feasible to undertake a subregional characterization of the space–time rainfall process, resulting in the parameters presented in Table 1. The obtained parameters reveal a significantly large variability in the rainfall dynamics across various portions of southern Italy. The observed probability distributions of the rainfall cell areas are depicted in Figure 5, where the empirical probability density function (pdf) is fitted with an exponential distribution. It is worth noting that Regions 1 and 2 are relatively small, limiting the ability to achieve a robust characterization of this probability distribution.

The application of the model over southern Italy is shown in Figure 6, where the differences in the probability distributions obtained in the six different zones are clearly visible. Figure 6 depicts, in a Gumbel plot, the cumulative probability distributions of the annual rainfall maxima recorded in each of the six zones of the present study. The STMM probability distribution is depicted with a dashed blue line, and it is compared with the regional TCEV probability distribution obtained following the procedure suggested by Fiorentino, Versace, and Rossi (1985). Considering that the regional procedure is based on the

TABLE 1 | Parameters of the rainfall Poisson process estimated on each of the six zones identified in the present study.

Zone	Description of the zone	λ_r (N/year/km)	E[DA] (km^2)	λ (N/year)	E[Y] (mm)
1	The Park of Matese	0.0014	269.6	0.3774	143.7
2	The Sorrento Peninsula	0.0010	275.7	0.2757	140.8
3	The Gulf of Policastro	0.0008	431.8	0.3454	144.5
4	Ionian coast of Calabria	0.0002	2204.3	0.4409	168.2
5	Internal area	0.0001	227.3	0.0227	134.4
6	Coastal area without significant relief	0.0003	330.6	0.0992	140.0

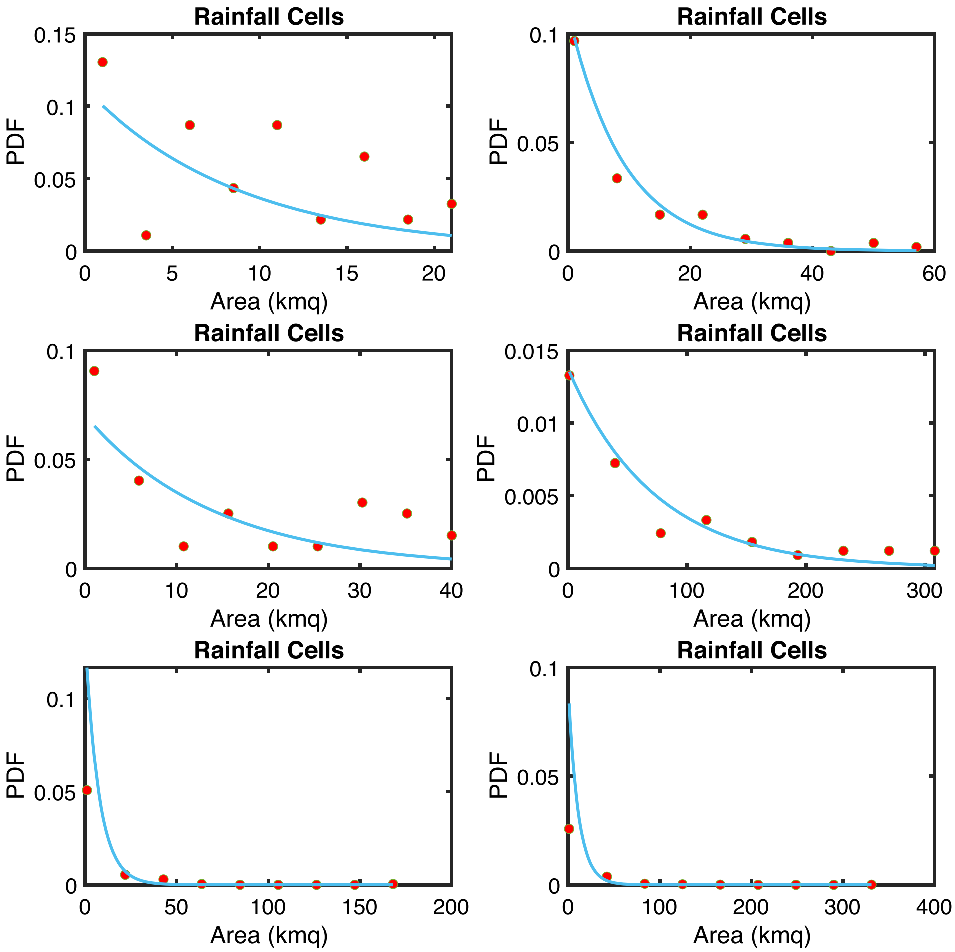

FIGURE 5 | Probability density functions of the size of the rainfall cells derived for each of the six zones identified in southern Italy.

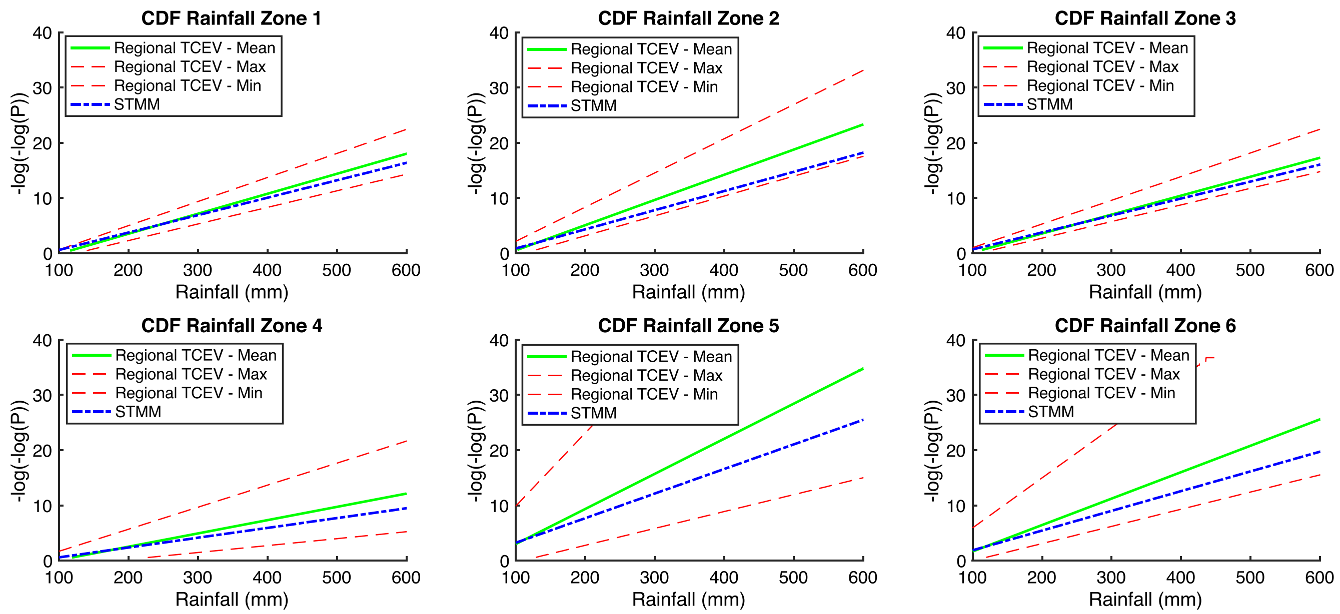

FIGURE 6 | Comparison of the cumulative probability distributions of the rainfall above the threshold of 112 mm obtained with the STMM (blue dashed line) in the 6 Zones identified in the present manuscript. The distribution has been compared with the regional TCEV, which provide a range of solutions within the selected zones. The central line refers to the average distribution (green solid line) and the minimum and maximum of the area (red dashed line).

TABLE 2 | Rainfall quantiles were estimated using the proposed methodology for the six regions of interest with three different methods: at-site, regional and STMM methods. It is worth noting that for on-site estimations, the values represent averages over the respective areas, with the range in parentheses indicating the minimum and maximum values obtained for each area.

Description of the zone	**At site estimations with GEV distribution**			
	h (mm) at T = 100 years	**h (mm) at T = 200 years**	**h (mm) at T = 500 years**	**h (mm) at T = 1000 years**
1 – The Park of Matese	185 (122–267)	192 (128–338)	200 (136–462)	206 (140–585)
2 – The Sorrento Peninsula	210 (135–304)	236 (143–368)	274 (153–476)	308 (159–580)
3 – The Gulf of Policastro	278 (249–308)	324 (289–359)	396 (352–440)	460 (409–511)
4 – Ionian coast of Calabria	300 (198–422)	335 (217–481)	385 (241–567)	426 (258–636)
5 – Internal area	126 (79–197)	139 (83–235)	158 (84–309)	173 (85–385)
6 – Coastal areas without significant relief	178 (122–267)	203 (128–338)	239 (136–462)	270 (140–585)
Description of the zone	Regional estimations with the TCEV distribution			
1 – The Park of Matese	240 (200–290)	261 (217–315)	290 (241–350)	312 (259–377)
2 – The Sorrento Peninsula	212 (156–269)	230 (169–292)	256 (188–324)	275 (202–349)
3 – The Gulf of Policastro	235 (188–268)	255 (204–291)	284 (227–323)	305 (244–348)
4 – Ionian coast of Calabria	246 (148–473)	267 (161–514)	297 (179–570)	320 (193–614)
5 – Internal area	128 (61–267)	140 (67–290)	155 (74–323)	167 (80–347)
6 – Coastal areas without significant relief	161 (85–248)	175 (92–269)	194 (102–299)	209 (110–322)
	STMM—space–time maxima model			
1 – The Park of Matese	226.9	249	278.1	300.1
2 – The Sorrento Peninsula	207.5	227.6	254.1	274.1
3 – The Gulf of Policastro	227.1	249.8	279.7	302.3
4 – Ionian coast of Calabria	324.8	364	415.6	454.7
5 – Internal area	130.3	146	166.6	182.2
6 – Coastal areas without significant relief	176.1	195.6	221.3	240.7

definition of a regional frequency curve of the normalized variable represented by the rainfall depth divided by the local mean, the final result produces a range of possible functions that reflect the range of variability of the means. Therefore, the TCEV is represented as a reference mean and two bounds associated with the minimum and maximum of the zone. The proposed STMM is always between the average and the maximum of each zone. It is noteworthy that the rainfall quantiles on the Ionian coastline of the Calabria region (Zone 4) are significantly higher than those in other areas.

5 | Discussion

The present manuscript offers an approach for the estimate of the probability distribution for extraordinary events based on a space–time modelling scheme. In certain applications, predicting extraordinary events holds greater significance and relevance for enhancing current hydrological estimation methods. This explorative study presented here provided interesting results that seems to be reliable in terms of prediction and characterization of extraordinary events. The methodology introduced herein has significant potential if a good space–time representation of rainfall extremes becomes available over a long temporal window.

The concept of extrapolating the probability distribution of the second component of annual maxima directly from the space–time characteristics of rainfall events overcomes the classical limitations of traditional approaches, such as point-scale estimations or even regional models. In fact, an extraordinary event has a relatively low probability of being recorded in a single rain gauge, expanding the study to include the spatial patterns of extraordinary rainfall events can enhance the accuracy of parameter estimation and improve the reliability of predictions.

At-site statistical inference may be significantly distorted by the presence of one or a few extraordinary events, which may occur with the same probability in nearby locations. Therefore, the resulting probability distributions may produce significant bias in the estimation of values at higher return periods. This difference has been highlighted in the analysis presented herein, where the STMM provides specific large-scale estimations, while other methods provide estimations that are always linked to the local observations. Such differences are highlighted in Figure 6 and Table 2, where the comparison of the results of the STMM method with at-site estimations of rainfall maxima and regional estimations applied over the available stations within each of the six zones identified in the study are presented. It is important to note that the comparison was possible between the mean value of the estimations, along with a range of values (minimum and maximum), obtained with the at-site estimations using the GEV or TCEV probability distributions.

The two methods exhibit overall agreement, particularly concerning the mean values of the rainfall quantiles estimated across each homogeneous area. However, both local and regional estimates reveal significant variability in the extrapolated quantiles for the large return period utilized in the present study. The observed dispersion, especially in the upper bounds of the estimations, is attributed to the limited length of the time series considered, spanning from 35 to 50 years of observations. This variability is generally mitigated by regional estimates, which closely align with the values provided by the STMM method.

Even though the proposed method has a very simple schematization, it has been able to correctly capture the order of magnitude of potential extreme events recorded over the area. The results cannot coincide because the two methods are based on significantly different methodological approaches, but it is interesting to note that the estimations of the quantiles obtained with the STMM are very close to the range of values obtained with the at-site and regional estimations. This implies that the estimation of extreme events for higher return periods may be obtained by focusing only on the extraordinary values. Additionally, it is interesting to note that the largest differences between the two estimations are observed over the smallest zones, which may induce a sampling issue.

The hypothesis of clustering regions assumes that large areas have constant characteristics, leading to significant differences at regional boundaries, which may be somewhat unrealistic. In this context, the methodology introduced by Cowpertwait, Kilsby, and O'Connell (2002) offers an improvement on the Cox and Isham (1988) model by incorporating the spatial distribution of rainfall parameters. This approach addresses the impact of spatial variations on extremes and other rainfall statistics and may represent a viable strategy to improve the technical applicability of STMM.

6 | Conclusion

This study addresses the challenge of characterizing extraordinary rainfall events, which are often challenging to observe accurately with traditional point measurements. Through the application of a space–time Poisson model, the research successfully overcomes the limitations posed by sparse rain gauge networks. The model, based on circular-shaped rainfall cells with random depth, focuses specifically on extraordinary events associated with larger meteorological phenomena, transcending local landscape heterogeneity.

The investigation conducted across southern Italy reveals significant regional differences in the dynamics of extraordinary events, with six distinct zones identified based on their frequency. The calibration of model parameters using a simple mathematical representation allows for the estimation of a regional probability distribution defined across homogeneous zones. This approach proves valuable in providing a more comprehensive understanding of extreme events, overcoming the constraints of point observations by offering a distribution that pertains to entire regions rather than individual points.

Acknowledging the inherent limitations of the rainfall data utilized for characterizing extraordinary events, one potential solution is to incorporate long-term radar observations. This approach aims to offer a more refined representation of extraordinary phenomena. The undertaking of such a task as a future research activity necessitates time-consuming calibration processes; nonetheless, it has the potential to signify a significant advancement in this field.

Despite the challenges, the proposed study stands as a promising starting point for quantitatively characterizing the probability distribution of extraordinary rainfall events. The alignment of estimated quantiles of rainfall with the upper bounds of the probability distribution underscores the model's effectiveness in capturing and predicting extreme events.

In summary, the study introduces a novel approach to the analysis of extraordinary rainfall events, leveraging a space–time modelling scheme to enhance our understanding of their occurrence and characteristics across distinct regions. The identified zones and their associated dynamics contribute valuable insights, laying the groundwork for further refinement and exploration in the field of hydrological predictions.

Dedication

This small project has been on my mind for several years, and I finally found the energy and motivation to complete it during Christmas, considering the approaching deadline for the special issue dedicated to Ignacio. Although I never had the chance to discuss it with my mentor, Ignacio, I am confident he will be curious to learn how his thoughts have evolved over time. I hope this work can serve as a useful reminder of his genius and ground-breaking way of thinking.

Acknowledgements

This study was carried out within the RETURN Extended Partnership and received funding from the European Union Next-Generation EU (National Recovery and Resilience Plan - NRRP, Mission 4, Component 2, Investment 1.3 - D.D. 1243 2/8/2022, PE0000005). Open access publishing facilitated by Universita degli Studi di Napoli Federico II, as part of the Wiley - CRUI-CARE agreement.

Data Availability Statement

The data that support the findings of this study are openly available in Zenodo at https://www.doi.org/10.5281/zenodo.10465589, reference number 10465589.

References

Avino, A., L. Cimorelli, P. Furcolo, et al. 2024. "Are Rainfall Extremes Intensifying in Southern Italy?." *Journal of Hydrology* 631: 130684.

Avino, A., S. Manfreda, L. Cimorelli, and D. Pianese. 2021. "Trend of Annual Maximum Rainfall in Campania Region (Southern Italy)." *Hydrological Processes* 35, no. 12: e14447. https://doi.org/10.1002/hyp.14447.

Avino, A., D. Pianese, and S. Manfreda. 2024. "Reconstructed Sub-Daily Rainfall Annual Maxima for Southern Italy." https://doi.org/10.5281/zenodo.10465589.

Bárdossy, A., and F. Anwar. 2023. "Why Do our Rainfall–Runoff Models Keep Underestimating the Peak Flows?." *Hydrology and Earth System Sciences* 27: 1987–2000. https://doi.org/10.5194/hess-27-1987-2023.

Benito, G., Y. Sanchez-Moya, A. Medialdea, et al. 2020. "Extreme Floods in Small Mediterranean Catchments: Long-Term Response to Climate Variability and Change." *Water* 12, no. 4: 1008.

Beran, M., J. R. M. Hosking, and N. Arnell. 1986. "Comment on Two Component Extreme Value Distribution for Flood Frequency Analysis." *Water Resources Research* 22: 263–266.

Boni, G., A. Parodi, and R. Rudari. 2006. "Extreme Rainfall Events: Learning From Raingauge Time Series." *Journal of Hydrology* 327, no. 3–4: 304–314.

Campos-Aranda, D. F. 2022. Regional flood frequencies analysis based on the TCEV distribution in Hydrological Region No. 10 (Sinaloa), Mexico.

Caporali, E., V. Chiarello, and A. Petrucci. 2018. "Regional Frequency Analysis and Geoadditive Modeling for Design Storm Estimates in the Arno River Basin (Italy)." *Environmental and Ecological Statistics* 25, no. 1: 31–52.

Chen, Y., A. Paschalis, L.-P. Wang, and C. Onof. 2021. "Can We Estimate Flood Frequency With Point-Process Spatial Temporal Rainfall Models?." *Journal of Hydrology* 600: 126667. https://doi.org/10.1016/j.jhydrol.2021.126667.

Claps, P., and M. Fiorentino. 2001. Rapporto di sintesi per la regione Basilicata (bacini del versante ionico).

Connell, R. J., and C. P. Pearson. 2001. "Two-Component Extreme Value Distribution Applied to Canterbury Annual Maximum Flood Peaks." *Journal of Hydrology. New Zealand* 40, no. 12: 105–127.

Cowpertwait, P. S. 1995. "A Generalized Spatial-Temporal Model of Rainfall Based on a Clustered Point Process." *Proceedings of the Royal Society of London. Series a: Mathematical and Physical Sciences* 450, no. 1938: 163–175.

Cowpertwait, P. S. P. 1994. "A Generalized Point Process Model for Rainfall." *Proceedings of the Royal Society of London, Series a* 447, no. 1929: 23–37.

Cowpertwait, P. S. P. 1998. "A Poisson-Cluster Model of Rainfall: Some High-Order Moments and Extreme Values." *Proceedings of the Royal Society of London, Series A* 454, no. 1971: 885–898. https://doi.org/10.1098/rspa.1998.0191.

Cowpertwait, P. S. P., C. G. Kilsby, and P. E. O'Connell. 2002. "A Space-Time Neyman-Scott Model of Rainfall: Empirical Analysis of Extremes." *Water Resources Research* 38, no. 8: 6–1.

Cowpertwait, P. S. P., and P. E. O'Connell. 1997. "A Regionalised Neyman-Scott Model of Rainfall With Convective and Stratiform Cells." *Hydrology and Earth System Sciences* 1: 71–80. https://doi.org/10.5194/hess-1-71-1997.

Cowpertwait, P. S. P., P. E. O'Connell, A. V. Metcalfe, and J. A. Mawdsley. 1996. "Stochastic Point Process Modelling of Rainfall. I. Single-Site Fitting and Validation, II. Regionalisation and Disaggregation." *Journal of Hydrology* 175, no. 1–4: 17–65.

Cox, D. R., and V. Isham. 1988. "A Simple Spatial-Temporal Model of Rainfall." *Proceedings of the Royal Society of London, Series A* 415, no. 1849: 317–328.

De Luca, D. L., and F. Napolitano. 2023. "A User-Friendly Software for Modelling Extreme Values: EXTRASTAR (EXTRemes Abacus for STAtistical Regionalization)." *Environmental Modelling & Software* 161: 105622.

de Vos, L. W., H. Leijnse, A. Overeem, and R. Uijlenhoet. 2019. "Quality Control for Crowdsourced Personal Weather Stations to Enable Operational Rainfall Monitoring." *Geophysical Research Letters* 46, no. 15: 8820–8829.

Diez-Sierra, J., S. Navas, and M. del Jesus. 2023. "NEOPRENE v1.0.1: A Python Library for Generating Spatial Rainfall Based on the Neyman–Scott Process." *Geoscientific Model Development* 16, no. 17: 5035–5048. https://doi.org/10.5194/gmd-16-5035-2023.

Emmanouil, S., A. Langousis, E. I. Nikolopoulos, and E. N. Anagnostou. 2022. "The Spatiotemporal Evolution of Rainfall Extremes in a Changing Climate: A CONUS-Wide Assessment Based on Multifractal Scaling Arguments." *Earth's Future* 10, no. 3: e2021EF002539.

Fiorentino, M., P. Versace, and F. Rossi. 1985. "Regional Flood fre-Quency Estimation Using the two-Component Extreme Value Distribu-Tion." *Journal of Hydrology Science* 30, no. 1: 51–64.

Fowler, H. J., H. Ali, R. P. Allan, et al. 2021. "Towards Advancing Scientific Knowledge of Climate Change Impacts on Short-Duration Rainfall Extremes." *Philosophical Transactions of the Royal Society a* 379, no. 2195: 20190542.

Goudenhoofdt, E., L. Delobbe, and P. Willems. 2017. "Regional Frequency Analysis of Extreme Rainfall in Belgium Based on Radar Estimates." *Hydrology and Earth System Sciences* 21: 5385–5399. https://doi.org/10.5194/hess-21-5385-2017.

Hanson, L. S., and R. Vogel. 2008. "The Probability Distribution of Daily Rainfall in the United States." In *World Environmental and Water Resources Congress 2008: Ahupua'A*, 1–10. Reston: American Society of Civil Engineers.

Hosking, J. R. M., and J. R. Wallis. 1988. "The Effect of Intersite Dependence on Regional Frequency Analysis." *Water Resources Research* 241: 588–600.

Isham, V., D. R. Cox, I. Rodríguez-Iturbe, A. Porporato, and S. Manfreda. 2005. "Representation of Space-Time Variability of Soil Moisture." *Proceedings of the Royal Society a: Mathematical, Physical and Engineering Sciences* 461, no. 2064: 4035–4055. https://doi.org/10.1098/rspa.2005.1568.

Istok, J. D., and L. Boersma. 1989. "A Stochastic Cluster Model for Hourly Precipitation Data." *Journal of Hydrology* 106: 257–285.

Jenkinson, A. F. 1955. "The Frequency Distribution of the Annual Maximum (Or Minimum) Values of Meteorological Elements." *Quarterly Journal of the Royal Meteorological Society* 81: 158–171.

Kavvas, M. L., and J. W. Delleur. 1981. "A Stochastic Cluster Model of Daily Rainfall Sequences." *Water Resources Research* 17, no. 4: 1151–1160. https://doi.org/10.1029/WR017i004p01151.

Lima, A. O., G. B. Lyra, M. C. Abreu, J. F. Oliveira-Júnior, M. Zeri, and G. Cunha-Zeri. 2021. "Extreme Rainfall Events Over Rio de Janeiro State, Brazil: Characterization Using Probability Distribution Functions and Clustering Analysis." *Atmospheric Research* 247: 105221.

Manfreda, S., D. Miglino, K. C. Saddi, et al. 2024. "Advancing Hydrological Monitoring Using Image-Based Techniques: Challenges and Opportunities." *Hydrological Sciences Journal* 69, no. 6: 657–677. https://doi.org/10.1080/02626667.2024.2333846.

Manfreda, S., and I. Rodrìguez-Iturbe. 2006. "On the Spatial and Temporal Sampling of Soil Moisture Fields." *Water Resources Research* 42: W05409. https://doi.org/10.1029/2005WR004548.

Nordbotten, J. M., I. Rodriguez-Iturbe, and M. A. Celia. 2006. "Non-uniqueness of Evapotranspiration Due to Spatial Heterogeneity of Plant Species." *Proceedings of the Royal Society A: Mathematical, Physical and Engineering Sciences* 462, no. 2072: 2359–2371.

Onof, C., R. E. Chandler, A. Kakou, P. Northrop, H. S. Wheater, and V. Isham. 2000. "Rainfall Modelling Using Poisson-Cluster Processes: A Review of Developments." *Stochastic Environmental Research and Risk Assessment* 14: 384–411.

Overeem, A., T. A. Buishand, and I. Holleman. 2009. "Extreme Rainfall Analysis and Estimation of Depth-Duration-Frequency Curves Using Weather Radar." *Water Resources Research* 45, no. 10: W10424. https://doi.org/10.1029/2009WR007869.

Peleg, N., F. Marra, S. Fatichi, A. Paschalis, P. Molnar, and P. Burlando. 2018. "Spatial Variability of Extreme Rainfall at Radar Subpixel Scale." *Journal of Hydrology* 556: 922–933.

Pelosi, A., P. Furcolo, F. Rossi, and P. Villani. 2020. "The Characterization of Extraordinary Extreme Events (EEEs) for the Assessment of Design Rainfall Depths With High Return Periods." *Hydrological Processes* 34, no. 11: 2543–2559.

Ramirez, J. A., and R. L. Bras. 1985. "Conditional Distributions of Neyman–Scott Models for Storm Arrivals and Their Use in Irrigation Scheduling." *Water Resources Research* 21, no. 3: 317–330.

Rodriguez-Iturbe, I., D. R. Cox, and V. Isham. 1987. "Some Models for Rainfall Based on Stochastic Point Processes." *Proceedings of the Royal Society of London, Series a* 410: 269–288.

Rodríguez-Iturbe, I., V. Isham, D. R. Cox, S. Manfreda, and A. Porporato. 2006. "Space-Time Modeling of Soil Moisture: Stochastic Rainfall Forcing With Heterogeneous Vegetation." *Water Resources Research* 42: W06D05. https://doi.org/10.1029/2005WR004497.

Romera, R., M. Á. Gaertner, E. Sánchez, M. Domínguez, J. J. González-Alemán, and M. M. Miglietta. 2017. "Climate Change Projections of Medicanes With a Large Multi-Model Ensemble of Regional Climate Models." *Global and Planetary Change* 151: 134–143.

Romero, R., and K. Emanuel. 2013. "Medicane Risk in a Changing Climate." *Journal of Geophysical Research: Atmospheres* 118, no. 12: 5992–6001.

Rossi, F., M. Fiorentino, and P. Versace. 1984. "Two-Component Extreme Value Distribution for Flood Frequency Analysis." *Water Resources Research* 20, no. 7: 847–856.

Schaefer, M. G. 1990. "Regional Analyses of Precipitation Annual Maxima in Washington State." *Water Resources Research* 26, no. 1: 119–131. https://doi.org/10.1029/WR026i001p00119.

Thompson, S. E., M. Sivapalan, C. J. Harman, et al. 2013. "Developing Predictive Insight Into Changing Water Systems: Use-Inspired Hydrologic Science for the Anthropocene." *Hydrology and Earth System Sciences* 17, no. 12: 5013–5039.

Totaro, V., A. Gioia, G. Kuczera, and V. Iacobellis. 2024. "Modelling Multidecadal Variability in Flood Frequency Using the two-Component Extreme Value Distribution." *Stochastic Environmental Research and Risk Assessment* 38, 2157–2174. https://doi.org/10.1007/s00477-024-02673-8.

Versace, P., E. Ferrari, S. Gabriele, and F. Rossi. 1989. Valutazione delle Piene in Calabria. Cosenza. Italy: CNR-IRPI e GNDCI, Geodata, 30, P. Benvenuto.

Waymire, E., and V. K. Gupta. 1981. "The Mathematical Structure of Rainfall Representation: A Review of Stochastic Rainfall Models." *Water Resources Research* 17, no. 5: 1261–1272.

Yang, P., and T. L. Ng. 2017. "Gauging Through the Crowd: A Crowd-Sourcing Approach to Urban Rainfall Measurement and Storm Water Modeling Implications." *Water Resources Research* 53, no. 11: 9462–9478.